Two-dimensional Fermi liquids sustain surprising roton-like plasmons beyond the particle-hole band

Ahmad Sultan, Henri Godfrin, Matthias Meschke, Hans J. Lauter, Helmut Schober, Helga Böhm, Robert Holler, Eckhard Krotscheck, Martin Panholzer

Two-dimensional Fermi liquids sustain surprising roton-like plasmons beyond the particle-hole band

A Sultan[1], H Godfrin[1], M Meschke[2], H-J Lauter[3,4], H Schober[3], H Böhm[5], R Holler[5], E Krotscheck[5] and M Panholzer[5]

[1] Institut Néel, CNRS et Université J. Fourier, BP 166, F-38042 Grenoble Cedex 9, France
[2] Low Temperature Laboratory, Aalto University, PO. Box 3500, 02015 TKK, Finland
[3] Institut Laue-Langevin, BP 156, 38042 Grenoble Cedex 9, France
[4] Oak Ridge National Laboratory, PO BOX 2008 MS6475, Oak Ridge TN 37831-6475, USA
[5] Institute for Theoretical Physics, Johannes Kepler University, A-4040 Linz, Austria

E-mail: henri.godfrin@grenoble.cnrs.fr

Abstract. Using inelastic neutron scattering, we have investigated the elementary excitations of an isotropic two-dimensional Fermi liquid, ^{3}He adsorbed on graphite. We provide in this article a detailed account of the principles and methods which allowed measuring for the first time inelastic spectra on a liquid monolayer of ^{3}He, a strong neutron absorber. We also summarise the results presented at this Conference, and review our recent experimental and theoretical work on this this interacting many-body system. At low wave-vectors, near the edge of the particle-hole band, a mode identified as the zero-sound excitation by comparison to our theoretical calculations, is found as predicted at energies much lower than in bulk ^{3}He. The mode enters the particle-hole band, where it undergoes Landau damping. Surprisingly, however, intensity is observed in the neutron spectra at wave-vectors larger than twice the Fermi wave-vector. This new branch is interpreted as the high wave-vector continuation of the zero-sound mode, in agreement with the theory. The results open new perspectives in the understanding of the dynamics of correlated fermions.

1. Introduction

The concept of elementary excitations was introduced by Landau to describe the low temperature behavior of quantum fluids: bosonic liquid ^{4}He and fermionic liquid ^{3}He. His elegant theory turned out to be the seed of the theoretical framework used presently to describe not only quantum fluids, but more generally condensed matter, nuclear and particle physics: i.e., all systems where strongly correlated matter plays an essential role. Quantum fluids ^{4}He and ^{3}He are still the unavoidable reference and benchmark: these simple monoatomic and isotropic systems display macroscopic quantum phenomena: Bose-Einstein condensation in liquid ^{4}He and a pure Fermi Liquid state with a spherical Fermi surface, Cooper pairing of fermions in liquid ^{3}He... Thanks to these extraordinary properties, theoretical predictions on topological excitations, particle physics and cosmologic effects can be tested in helium at very low temperatures, as we would do in a test tube! For this reason, the helium isotopes are named "model systems" and their properties are intensively investigated in low temperature laboratories.

In addition to thermodynamic studies, many efforts have been devoted by the neutron community to understand the dynamics of the strongly interacting quantum fluids. A milestone

for understanding correlated bosons was the observation of the "phonon-roton" collective mode of liquid ^{4}He, predicted by Landau [1] to explain the system's thermodynamics. For fermions, the situation is more complicated, since the spectrum hosts two types of modes: collective ("zero-sound" in ^{3}He, or "plasmon" in charged systems), and incoherent particle-hole (PH) excitations. Both are described by Landau's theory of Fermi liquids [2, 3] in the small wave-vector/ low energy region of the spectrum. At higher wave-vectors/energies, the collective mode enters the PH band, where it is strongly damped [2, 3]. It was thus believed that the dynamics at high wave-vectors is essentially incoherent.

We have recently reported preliminary inelastic neutron scattering data on a monolayer of liquid ^{3}He at very low temperatures [4, 5]. The most striking features were the observation of a zero-sound branch very close to the PH band and the presence of a roton-like excitation at high wave-vectors. We shall discuss in this Conference the neutron data showing the remarkable behaviour of this two-dimensional Fermi fluid, as well as the experimental techniques. Moreover, a new theoretical framework is proposed [6, 7] where we introduce intermediate states that are not describable by the quantum numbers of a single (quasi-)particle, leading to an accurate interpretation of the spectra measured for ^{3}He films. By exploring the dynamics of Fermi many-body systems in the region outside the scope of Landau's theory, we open new perspectives in the understanding of highly correlated fermions.

2. Fermi liquids

Fermi liquids constitute one of the most active research areas in condensed matter, and the reader is familiar with the fundamental publications: Landau's original papers, Pines and Nozières [2], Wilks [8], Fetter and Walecka [9], Dobbs [10] and other books. Liquid ^{3}He has been investigated in detail, owing to the simplicity of its (spherical) Fermi surface, and the possibility to tune the interactions by simple changing the pressure from essentially zero (saturated vapour presure) to 3.4 Mpa. Thermodynamic results have completely confirmed Landau's phenomenological theory, but a microscopic theory is still lacking even at zero temperature. Several open questions are described in a remarkable article published by David Pines in Physics Today [11]. In the present article we are more particularly concerned by the dynamics of Fermi liquids. This information is contained in the dynamic structure factor, which has also been investigated in bulk liquid ^{3}He. This function of energy and wave-vector has been measured by neutron scattering; the main results are the direct observation of the particle-hole excitations as well as the zero-sound and the paramagnon collective mode, as predicted by Landau's theory of Fermi liquids.

2.1. Excitations in Fermi liquids

The fundamental excitation of a Fermi liquid at zero temperature is the creation of a particle-hole pair [2, 3]. The existence of the Fermi surface, and this is a fundamental topological effect, causes the excitations of the system to be confined to a region of the energy-momentum space, the particle-hole band (PHB). The boundaries of the PHB for a non-interacting system (Fermi gas) are given by the expression $\mathrm{E}/\mathrm{E}_F=(\mathrm{k}/\mathrm{k}_F)^2 \pm 2(\mathrm{k}/\mathrm{k}_F)$ where E_F is the Fermi energy $\mathrm{E}_F=\hbar^2\mathrm{k}^2/2m$, k_F is the Fermi wave-vector and m the mass of the ^{3}He atom. The Fermi wave-vector is simply calculated knowing the density and the dimensionality of the system.

Landau theory of Fermi liquids postulates the existence of "quasi-particles" having an effective mass m^* which is a measure for the density of states at the Fermi level. In liquid ^{3}He, m^*/m, as seen by heat capacity measurements, is substantially larger than one, and increases with pressure [3, 8]. One could expect the PHB to shift to lower energies by a substantial amount, due to the increased effective mass. However, in the energy investigated here this does not happen: the Landau picture is only valid for very small energies and wave-vectors.

According to Landau's theory, two collective modes are present in a Fermi liquid [2, 3]: a collective oscillation of the Fermi sphere (zero-sound collective density wave), and a spin wave

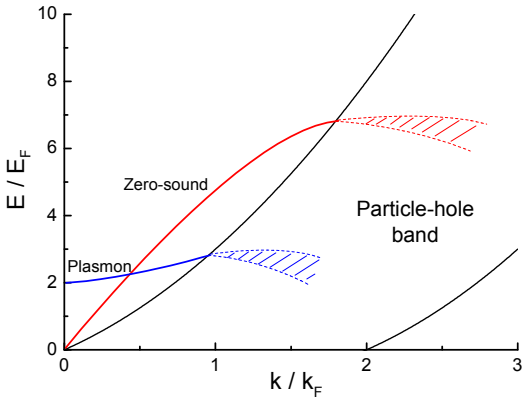

Figure 1. Schematic representation of the elementary excitations of a Fermi liquid. The spectrum displays an incoherent particle-hole band, and collective modes (zero-sound in a neutral Fermi liquid, like ^{3}He, or plasmons in a charged system, like the conduction electrons of a metal).

(paramagnon mode). Zero-sound has been detected first at low wave-vectors and very low temperatures by ultrasonic techniques. More recently, several neutron scattering investigations [3, 12, 13, 14] have been performed at wave-vectors on the order of k_F. At relatively low wave-vectors, zero-sound is observed as a well-defined mode with a linear dispersion relation, located above the PHB. It displays then a negative curvature, finally entering the PHB. There, the zero-sound branch becomes very broad, due to Landau damping: it decays into incoherent PH excitations [2, 3]. In electronic systems, the mode also exists, although its dispersion relation is modified due to the charged nature of the fermions. The collective electronic density mode is named "plasmon" [2]. A gap is present at small wave-vectors, but the high wave-vector behaviour is silmilar to that of liquid ^{3}He zero sound, the dispersion relation apparently finishes within the particle-hole band. We shall see that this is not necessarily true for two-dimensional systems.

3. Two-dimensional Fermi liquids

Two-dimensional liquid ^{3}He has been investigated using thermodynamic techniques by many research groups. Pionnering heat capacity investigations on liquid ^{3}He adsorbed on graphite were realised in Seattle [15], Grenoble (neutrons and NMR) [16, 17, 18], Bell Laboratories (heat capacity) [19], and London (heat capacity, NMR) [20, 21], among others. The results display all the characteristics expected from Fermi liquids: the heat capacity is linear in temperature, and the magnetization does not depend on temperature near T=0. Since there is no critical point in 2D liquid ^{3}He, one can investigate systems whose densities range essentially from zero (Fermi gas) to very high densities, until the system solidifies, forming a "commensurate solid" with respect to the graphite, or to the underlying adsorbed layer. The effect of the interactions appears, following Landau's theory, through an enhancement of the thermodynamic properties with respect to those of the Fermi gas. According to heat capacity and magnetization measurements, the effective mass increases as a function of density from $m^* = m$ to very large values, substantially larger than in bulk liquid ^{3}He.

Before our experiments, nothing was known experimentally about the dynamics of two-dimensional liquid ^{3}He. The measurements brought several surprises. The first one was the observation of a substantial change of the zero-sound mode, found to be at much lower energies that in bulk liquid ^{3}He. The main challenge, however, was the observation of substantial intensity

in the inelastic structure factor at wave-vectors on the order of $2k_F$, indicating the emergence of a new excitation branch beyond the particle hole continuum. We present in the following sections the principles and methods of the experiment, we show typical results of the neutron scattering measurements, and we discuss finally the associated theoretical developments.

4. Experimental details

The *principle* of the experiment is simple. The excitations created in a liquid ^{3}He film are measured by inelastic neutron scattering. The liquid ^{3}He film of atomic thickness (submonolayer characterised by a carefully determined areal density) is adsorbed on an exfoliated graphite substrate of relatively large surface area. The substrate is enclosed in an aluminium experimental cell. The system is cooled by a dilution refrigerator to temperatures well below 100 mK, where k_BT is much lower than characteristic excitation energies. At such low temperatures, the pressure of the ^{3}He gas in equilibrium with the adsorbed ^{3}He film is essentially zero, and therefore all the ^{3}He present in the cell is adsorbed on the substrate.

The recorded neutron spectra correspond to neutrons reaching a set of detectors placed in a horizontal plane (scattering angle) at different times (time-of-flight technique to determine their energy). The neutron spectra reveal the creation of excitations in the ^{3}He film. This experiment requires a detailed data analysis, which involves a careful subtraction of the background signal due to the substrate, the experimental cell and the instrument. We describe in the following subsections the experimental set-up, the measuring techniques, as well as the details of the data analysis.

4.1. Neutron scattering on ^{3}He samples

The neutron scattering inelastic measurements were performed at the Institut Laue-Langevin (ILL - Grenoble) on the time-of-flight spectrometer IN6, situated on the cold neutron guide of the high flux reactor. IN6 is a time-focussing time-of-flight spectrometer designed for quasi-elastic and inelastic scattering for incident wave-lengths in the range of 0.4 to 0.6 nm. Experiments were performed at two wave-lengths: at 0.51 nm giving acess to the main part of the interesting energy-momentum range, and 0.41 nm in order to extend the range to higher energies and momenta. The energy resolution for a wave-length of 0.51 nm is on the order of 0.08 meV, increasing with the wave-vector up to 0.12 meV. At the smaller incident wave-length (0.41 nm), the resolution is about twice these values. A large number (337) of elliptical ^{3}He detectors cover the scattered neutrons angular range from 11.9 to 113 degrees. This corresponds, for elastic scattering, to wave-vectors in the range up to 20.5 nm^{-1} at an incident wave-length of 0.51 nm, and 24 nm^{-1} at an incident wave-length of 0.41 nm). The useful energy range is 0.1 to 2 meV (0.2 to 4 mev) repectively, for the two different wave-lengths.

The energy-momentum range of IN6 is particularly well adapted to the investigation of quantum fluids dynamics [22, 23, 24]. In particular, this instrument was used by Scherm and coworkers for bulk liquid ^{3}He studies [13, 14]. These experimental data have been very useful as a reference for the analysis of the results obtained on the two-dimensional samples.

One of the major difficulties encountered in measuments on ^{3}He is the very large absorption cross section of this isotope [3, 12, 14]. At the long wavelenghts needed for the inelastic measurements, the neutron penetration is on the order of a tenth of a millimetre in bulk liquid ^{3}He. For this reason, a high flux (the flux at the sample is on the order of 10^5 cm^{-2} sec^{-1}) and very long measuring times (about 20 hours) are necessary in order to collect a few neutron counts on each detector. The sample geometry and environment must therefore be carefully studied to reduce the background.

The experiments presented here on liquid ^{3}He films share with bulk liquid ^{3}He measurements the difficulties discussed above: high absorption and small signal. They present additional experimental complications, the most obvious one being the necessity of a solid substrate onto

which the liquid ^{3}He monoatomic film is adsorbed. We use exfoliated graphite, as decribed below. The substrate introduces intense elastic scattering, in particular at Q=0, and at the graphite (0002) reflection; a phonon branch emerging from this Bragg peak also contaminates the signal. The graphite sample is oriented with the (0002) direction normal to the scattering plane, and therefore, the Bragg reflection should not occur in the scattering plane. However, the mosaic spread of the substrate leads to a Bragg peak in the scattering plane at 18.767nm^{-1}. In addition, instrumental background as well as neutrons incoherently scattered on impurities resulting from the graphite exfoliation procedure lead to quasielastic scattering. These spurious signals are not negligible, compared to the small number of counts originating from the ^{3}He inelastic scattering we want to measure. For this reason, the spectra of two-dimensional ^{3}He cannot be exploited at small energies.

Since the adsorbed layer consists of ^{3}He, the neutron absorption of this isotope reduces the intensity of the signal. The absorption measured at the graphite Bragg peak is of about 20% in our experiments. Subtracting the background is thus a delicate task: one cannot simply use the measurement with the bare graphite substrate as background. A further complication is the modification of the graphite peak position, height and width due to the adsorption of one or more helium layers. This effect, due to the modification of the intereference pattern of a finite number of planes (additional planes are introduced by the helium adsorption), is well known in neutron surface studies (see references in [16, 24]). It is taken into account in the analysis by adequate fits of the peak shape and position; the procedure, performed for each Q value, is delicate and time consuming. A consistency check is made by comparing the peak evolution for samples of different areal density.

4.2. The exfoliated graphite substrate

Exfoliated graphite is an excellent substrate for the investigation of two-dimensional adsorbed systems [16, 17, 24]. It presents many advantages: homogeneous adsorption due to the presence of relatively large atomically flat platelets corresponding to the (0002) graphite planes; it can be cleaned by simple procedures (baking at a few hundred degrees), and pumping on the system is sufficient to remove most of the contamination of a sample exposed to air. For this reason, exfoliated graphite samples are used in neutron scattering, NMR and heat capacity investigations of two-dimensional ^{3}He, where the ultrahigh vacuum techniques used in many other surface studies cannot be applied.

Exfoliated graphite consists of natural graphite flakes, exfoliated using an intercalation and a rapid heating procedure. The exfoliated material is then recompressed to form a self-sustaining material. Diverse levels of exfoliation are found in commercially available materials (Grafoil, Papyex...). They are characterised by their specific surface area ($20\,\text{m}^2$/gram for Grafoil), by the size of the atomically flat regions (the coherence length is typically 20 nm), by the mosaic spread of the crystallites orientation (typically 30 degrees), and by their thermal properties (in particular the thermal conductivity at low temperatures) [16].

The choice of the substrate is dictated by several considerations. A large specific surface area is in principle convenient, since the signal is proportional to the amount of adsorbed gas. However, the strong neutron absorption of ^{3}He introduces a severe limitation. A Grafoil sample covered with ^{3}He would absorb all the beam within a thickness of a few millimetres. For this reason, we have chosen a ZYX-UCAR exfoliated graphite sample of smaller specific area ($2\,\text{m}^2$/gram), but of mucher higher quality in terms of coherence lenth (190 nm), mosaic spread (only 10 degrees) and thermal conductivity (the large graphite crystals ensure a more efficient heat transport). This sample has therefore the advantage to allow forming relatively large two-dimensional liquid ^{3}He regions, relatively well oriented within the neutron scattering plane, with a moderate total neutron absorption using a sample of dimensions comparable to the neutron beam size ($25\,\text{mm}\times 50\,\text{mm}$) [16]. In our experiments, a stack of ZYX graphite sheets of

dimensions $25\times25\times5\,\mathrm{mm}^3$, with a total height of 60 mm, was used.

4.3. Experimental cell and cryogenic set-up

The ZYX sample is placed in a copper holder consisting of two plates, at the top and bottom, connected by a copper rod for thermal purposes. The ZYX sheets are thermally connected to the copper plates by means of copper foils. These are located at the back side of the stack with respect to the neutron detectors. Copper to graphite bonding is achieved by thermal diffusion, at a temperature on the order of $800\,C$ for several hours, under secondary vacuum. This procedure also ensures the main cleaning (outgasing) of the graphite sample. Later on in the experimental procedure, pumping at room temperature will be sufficient to ensure that the full surface area of the sample is available for the sample absorption. The ZYX and its copper holder are placed in a thin walled aluminium cell. The top, made out of copper, is dismountable; an indium o-ring ensures that the cell is leak-tight. The copper top part is then bolted to the mixing chamber of a dilution refrigerator, providing a base temperature lower than 30 mK, determined by means of a calibrated carbon resistor thermometer. In the absence of the neutron beam, the sample temperature is essentially that of the mixing chamber. Opening the beam gives rise to a small temperature increase. This is not due to the absortion of neutrons by the ^{3}He film, since the energy released in the capture process is only 764 keV: heating originates in the absorption of gamma rays generated at the level of the instrument monochromator. Most of the power deposited in the experimental cell corresponds to absorption by the aluminium walls. The sample itself remains below 100 mK, which is sufficient for the purposes of this experiment. A vanadium sample is attached to the bottom of the cell. Measurements with this incoherent scatterer are used for the calibration of the relative efficiency of the 337 detectors. The dilution unit equipped with the sample cell are placed in the vacuum chamber of the instrument IN6. This allowed us to remove the room temperature vessel of the dilution unit, thus reducing the background. IN6 is also equipped of a helium filled box between the sample and the detectors, again reducing the background.

4.4. Adsorption isotherms system

In this experiment we handle small amounts of ^{3}He and ^{4}He gas, which must be accurately measured, both during the adsorption isotherm measurements and for the introduction of the helium sample. Typical quantities are on the order of $10\,\mathrm{cm}^3$ STP of gas. For this purpose we use a stainless steel manyfold (typical diameter 6 mm) including small dead-volume valves, 2 calibrated stainless steel volumes (a volume of about $1000\,\mathrm{cm}^3$ for the initial introduction of gas, and one of about $20\,\mathrm{cm}^3$ for small increments of the amount of gas). The pressure in the system is measured with a precision Baratron MKS pressure gauge (100 Torr range). The temperature of the room is carefully recorded, in order to convert the amounts of gas measured in the calibrated volumes to amounts of gas in STP conditions.

4.5. Calibration of the substrate surface area

The ZYX sample is characterized by ^{3}He and ^{4}He adsoption isotherms at 4.2 K [16]. This procedure, well known in surface science, yieds the "surface area" of the sample. The resulting figure, however, has to be used with caution. It is very accurate in the sense that the measurement can be repeated, for a given sample, obtaining the same result. Also, for samples of the same type, the ratio of the measured areas can be determined quite precisely. This allows a direct scaling of experimental results obtained in different laboratories. Comparing the adsorption isotherms, we can determine the amount of gas corresponding, for our sample, to a given density.

The phase diagram of ^{3}He adsorbed on graphite has been determined by heat capacity and NMR techniques as a function of the ^{3}He coverage and temperature [15, 16, 17, 18, 19]. These

measurements yield in particular the amount of gas needed to fill the $\sqrt{3}$ phase, the density of which is determined by the graphite in-plane lattice parameter as 6.366 atoms/nm^2. The "Commensurate surface area" A_c can therefore be determined from the ratio of the measured adsorption isotherm and that of another experiment where the commensurate phase coverage could be determined.

In addition, extensive neutron diffraction studies have been performed on the solid phases observed in the helium/graphite system: commensurate and incommensurate phases with respect to the graphite substrate have been observed [16, 17, 25]. The determination of the lattice parameter of these triangular phases gives immediately the specific area (nm^2/atom) for a given coverage. In previous experiments we have determined the amount of gas corresponding to the perfect filling of the commensurate phase using neutron diffraction on this sample to be 14.351 cm^3 of gas in standard conditions of temperature and pressure (STP: T=273.15 K and P=100 kPa). For comparison, a measurement performed using D_2, again on the same sample, gave the value 14.336 cm^3 STP for the $\sqrt{3}$ phase. One can then calculate the sample "commensurate area" A_c=59.73 m^2. This is the area that one should use for areal densities close to that of the $\sqrt{3}$ phase, at submonolayer coverages. At high coverages, however, adsorption of helium does not only take place at the atomically flat parts of the graphite platelets, but also at some places of weaker adsoption potential (defects, edges). The effective surface area near monolayer coverage is therefore somewhat larger than the "commensurate area" (which measures essentially the adsorption area of the homogeneous sites) [16, 17]. More specifically, we have determined by neutron diffraction on the same sample the commensurate area A_c, and also the effective area A_I which is available for adsorption at high coverages, on the dense incommensurate solid phase, in the vicinity of monolayer completion. The corresponding ratio of areas is 1.093, thus yielding an effective area for adsorption at high coverages A_I=65.3 m^2.

4.6. Preplating with ^{4}He

The results presented here correspond, as will be seen later, to a film of relatively high areal density: 4.7 atoms/nm^2. Such a density cannot be achieved at submonolayer coverages, since the fluids enters into a coexistence with the $\sqrt{3}$ phase at relatively low densities [16, 17]. In order to study a system where the interactions are strong, we have chosen to work with a fluid in the second layer, where the phase diagram offers a wider density range; although a commensurate phase also occupies a substantial part of the phase diagram, this effect only happens for densities of about 5.5 atoms/nm^2.

On the other hand, a dense ^{3}He solid first layer would have led to substantial neutron absorption. For this reason, we have used a ^{4}He complete monolayer. This isotope, due to its smaller zero point energy in the well formed by the adsoption potential and the interaction with neighbouring atoms, adsorbs preferentially with respect to ^{3}He, the lighter isotope. One can therefore engineer a bilayer system where the first layer consists of solid ^{4}He at high density, and the second layer of pure liquid ^{3}He. Preplating with ^{4}He also improves substantially the quality of the substrate, by smoothing out the imperfections of the bare graphite, in particular by filling the strong binding sites ("heterogeneities") which represent a few percent of the adsorbed first layer atoms. The high density first layer ^{4}He solid acts as a high quality, atomically smooth, substrate, onto which the ^{3}He layer can be deposited. The binding energy is much weaker than on the bare graphite: about 30 K compared to 140 K. The adsortion potential is nevertheless sufficiently strong, for experiments well below 1 Kelvin, to ensure that the motion of the adatoms is confined in the plane. The second layer ^{3}He fluid is therefore a practically ideal two-dimensional system, and confinement effects within the planes are very small, due to the large coherence length, increased with respect to the bare ZYX to values larger than 20 nm.

The amount of ^{4}He to be introduced to cover exactly the graphite by one atomic layer of ^{4}He can be determined using our neutron diffraction measurements on ^{4}He adsorbed on this

ZYX sample. Near monolayer completion the solid density is about 11.1 atoms/nm^2, and this number increases up to 11.63 atoms/nm^2 at very high coverages (maximum layer density) under the pressure of the additionally adsorbed atoms [16, 17]. The areal density of the complete ^{4}He first layer needed for the present experiment is found to be 11.3 atoms/nm^2, taking into account the compression due to the liquid ^{3}He second layer. The amount of ^{4}He gas introduced is 28.38 cm^3 of gas STP (standard temperature and pressure conditions, defined as T=273.15 K and P=100 kPa)

4.7. Two-dimensional ^{3}He sample

The amount of ^{3}He gas introduced in the cell is 11.03 cm^3 of gas STP. With the surface area of the substrate determined in the previous section, this corresponds to an areal density ρ_c=4.9 atoms/nm^2 in the commensurate coverage scale, and ρ_i=4.5 atoms/nm^2 in the incommensurate coverage scale. The first value is appropriate if the ^{3}He atoms of the liquid phase in the second layer explore only the homogeneous regions of the substrate, and the second value should be used if the fluid covers the whole area of the substrate, an effect favoured by the ^{4}He preplating. These values provide an upper and lower bound the actual density of the sample, which has therefore the value ρ=4.7±0.2 atoms/nm^2.

5. Measured neutron spectra

We show in this section results obtained on a two-dimensional liquid ^{3}He system of areal density ρ=4.7 atoms/nm^2 (see previous section). The Fermi wave-vector is obtained directly from the areal density; in two dimensions $k_F=\sqrt{2\pi\rho}$. The Fermi energy is $E_F=\hbar^2 {k_F}^2/2m$, and hence $E_F=\hbar^2\pi\rho/m$. The Fermi temperature is defined as $T_F=E_F/k_B$ (note than in 3D T_F is often defined including a 2/3 factor). With this notation, in the 2D system T_F [K]=0.5053 ρ [atoms/nm^2] and E_F [meV]=0.04355 ρ [atoms/nm^2]. For ρ=4.7±0.2 atoms/nm^2, k_F=5.43±0.12 nm^{-1}, E_F=0.204±0.009 meV

We present results for different scattering angles. Grouping of detectors provides a wave-vector resolution of 0.1 nm^{-1}. The subtraction of the large elastic signal of the cell (background) does not allow a precise determination of the spectrum for low energies, typically less than about 0.3 meV. We first discuss the "low wave-vector" region. We show in Figure 2 the spectrum obtained in our 2D system for a momentum transfer Q=5.5 nm^{-1}, comparable to the Fermi wave-vector. The most striking result is the absence of the collective mode observed in the bulk liquid at different pressures for energies of about 1 meV [3, 12, 13, 14]. Instead, we observe a mode whose energy is just above the PHB [4, 5]: the two-dimensional zero-sound collective mode, identified by the evolution of this signal in our data at different coverages (not shown here). Also, the mode corresponds well with theoretical results, which cover broad regions of the energy-momentum plane, including those where the experimental results are spoiled by the graphite background [26, 6, 7].

In Figure 3 we show the spectrum obtained for a momentum transfer Q= 11.5 nm^{-1}. It corresponds to the region dominated by the damping of excitations within the PHB [4, 5]. As expected, the signal is weak. However, one can clearly observe a broad mode, which corresponds to the damping of zero-sound within the PHB expected from theoretical calculations.

The behavior at higher wave-vectors is presented in Figure 4, where the momentum transfer is Q=16.5 nm^{-1}. The striking features are now the appearence of a large intensity peak (log scale!) at low energies, clearly *below* the PHB [4, 5]. Using data in the whole energy-momentum plane accessible with IN6 we have shown [5] that this intensity corresponds to the collective zero-sound mode reappearing beyond the PH continuum, at elevated wave-vectors.

The neutron spectra reflect the pronounced damping obtained within a rather well defined region of the energy-wave-vector plane, the particle-hole band. At this point, it is interesting

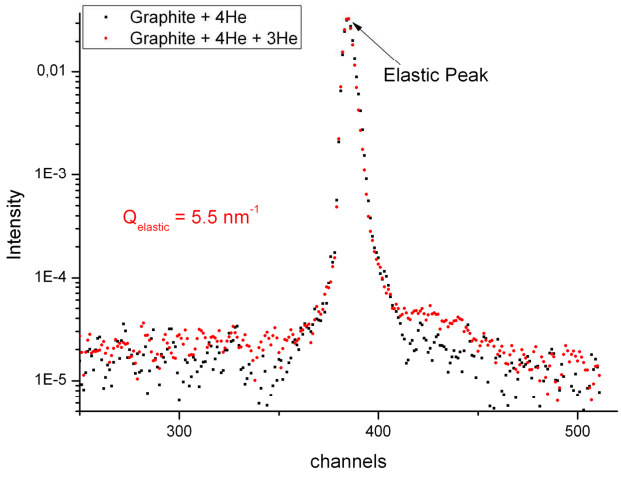

Figure 2. Time-of-flight inelastic neutron scattering spectrum measured at an angle of 25.5 degrees, corresponding to a wave-vector of 5.5 nm^{-1}. Note the logarithmic vertical (counts normalised to monitor) scale. A time channel corresponds to 9.625μsec. Squares are measurements of the background performed on the substrate preplated by a monolayer of ^{4}He. Circles correspond to the signal measured with the additional ^{3}He layer, after absorption corrections. A small signal is visible after the elastic peak, it corresponds to the creation of the zero-sound excitation at the upper edge of the particle-hole band.

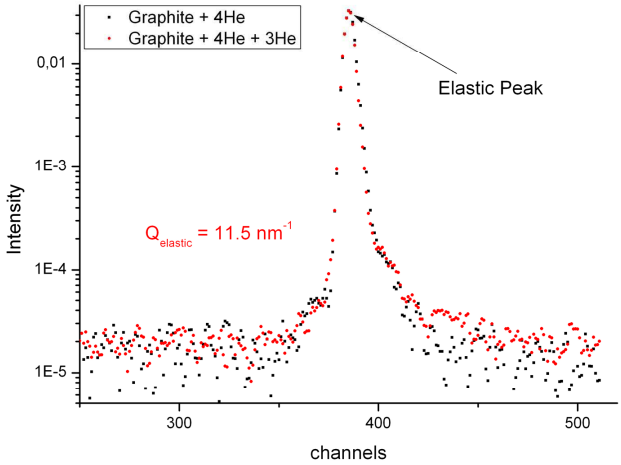

Figure 3. Time-of-flight inelastic neutron scattering spectrum measured at an angle of 55.3 degrees, corresponding to a wave-vector of 11.5 nm^{-1}. The weak signal after the elastic peak corresponds to the creation of highly damped zero-sound excitations inside the particle-hole band.

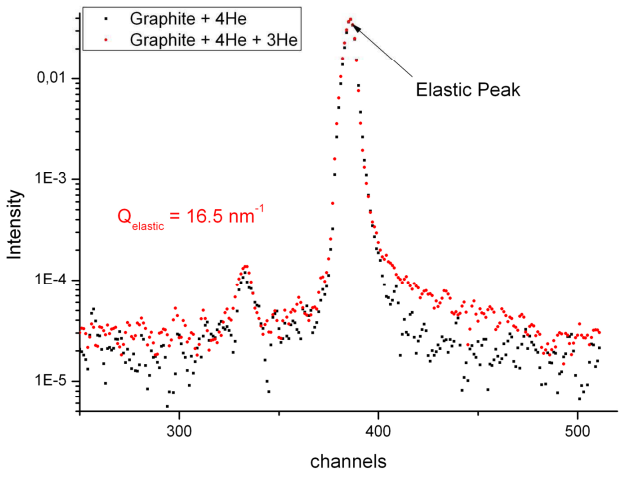

Figure 4. Time-of-flight inelastic neutron scattering spectrum measured at an angle of 84.1 degrees, corresponding to a wave-vector of 16.5 nm^{-1}. The rather intense signal observed after the elastic peak at very low excitation energies (short TOF times) corresponds to the creation of unexpected zero-sound excitations below the particle-hole band.

to reconsider the problem of the effective mass. The effective mass for a second-layer two-dimensional liquid ^{3}He film can be determined using the heat capacity data of Greywall [19] with the appropriate corrections for the coverage scale [18]. We obtain $m^* \approx 3.8$; for comparison, this is the effective mass observed in bulk liquid ^{3}He at a pressure of about 0.75 MPa. The PHB calculated using this value for the effective mass would be depressed to four time smaller energies, which is in contradiction with our data.

Including a large number of spectra like those displayed in the figures above, we obtained after a preliminary analysis [4], spectra which could be directly compared to the theory [4]. The complete set of data leads to an impressive agreement between the experiments and the dynamic many-body theory [5], presented during this Conference.

6. Conclusions

The inelastic neutron scattering, surface physics and low temperature techniques described here have allowed us to investigate directly the elementary excitations of a model 2D Fermi liquid, ^{3}He adsorbed on graphite. In spite of the technical difficulties of such an experiment, we were able to observe the zero-sound mode of a this interacting 2D Fermi Liquid in a large wave-vector range. At low wave-vectors the zero sound collective mode was found very close to the particle-hole band upper limit, substantially lower in energy than in the bulk, in agreement with theoretical calculations. The presence of the mode at high wave-vectors, damped in the region of coexistence with the incoherent particle-hole excitations, but well-defined for wave-vectors on the order of $2k_F$, is an important and surprising finding. The dynamic many-body theory developed by Krotscheck and coworkers [7] provides calculated spectra for our experimental conditions in excellent agreement with the experimental data. This effect is not specific to liquid ^{3}He, it should be observable in other two-dimensional non-localised many-body Fermi systems. This led us to propose a novel superconductivity mechanism mediated by high wave-vector density or spin-density fluctuations [5].

Acknowledgments
We acknowledge the financial support from the EU FRP7 low temperature infrastructure grant 228464 "Microkelvin", the Austrian-French grant FWF-ANR "High-Q Fermions" ANR-2010-INTB-403-01 and the CNRS-Air Liquide grant "Contrat de collaboration Recherche-Entreprise" 72B204/00.

References

[1] Landau L D 1947 *J. of Phys. Moscow* **11** 91
[2] Pines D and Nozières P 1966 *The Theory of Quantum Liquids* (New York : Benjamin)
[3] Glyde H R 1966 *Excitations in Liquid and Solid Helium* (Oxford : Clarendon Press)
[4] Godfrin H, Meschke M, Lauter H-J, Böhm H M, Krotscheck E and Panholzer M 2010 *J. of Low Temp. Phys.* **158** 147
[5] Godfrin H, Meschke M, Lauter H-J, Sultan A, Böhm H M, Krotscheck E and Panholzer M *to be published*
[6] Böhm H M, Krotscheck E, Panholzer M, Godfrin H, Lauter H-J and Meschke M 2010 *J. of Low Temp. Phys.* **158** 194
[7] Böhm H M , Holler R, Krotscheck E, Panholzer M 2010 *Phys. Rev. B* **82** 224505
[8] Wilks J 1967 *Liquid and Solid Helium* (Oxford : Clarendon Press)
[9] Fetter A L and Walecka J D 1971 *Quantum Theory of Many Particle Systems* (New York : McGraw-Hill)
[10] Dobbs E R 2001 *Helium Three* Oxford University Press
[11] Pines D 1981 *Physics Today* **34** 106
[12] Sköld K, Pelizzari C A, Kleb R and Ostrowski GE 1976 *Phys. Rev. Lett.* **37** 842
[13] Scherm R, Glucksberger K, Fak B, Sköld K, Dianoux A J, Godfrin H and Stirling W G 1987 *Phys. Rev. Lett.* **59** 217
[14] Glyde H R, Fak B, Dijk N H, Godfrin H, Glucksberger K and Scherm R 2000 *Phys. Rev. B* **61** 1421
[15] van Sciver S W and Vilches O E 1978 *Phys. Rev. B* **18** 285
[16] Godfrin H and Lauter H-J 1995 *Progress in Low Temp. Physics* Vol.XIV, Chapter 4, p.213-320, ed. W.P. Halperin, (Amsterdam : Elsevier Science B.V.)
[17] Godfrin H and Rapp RE 1995 *Advances in Physics* **44** 113
[18] Morhard K D, Bäuerle C, Bossy J, Bunkov Y M, Fisher S N and Godfrin H 1996 *Phys. Rev. B* **53** 2658
[19] Greywall D S 1990 *Phys. Rev. B* **41** 1842
[20] Casey A, Patel H, Nyéki J, Cowan B P and Saunders J 2003 *Phys. Rev. Lett.* **90** 115301
[21] Neumann M, Nyéki J, Cowan B P and Saunders J 2007 *Science* **317** 1356
[22] Stunault A, Andersen K H, Blanc Y, Fak B, Godfrin H, Guckelsberger K and Scherm R 1992 *Physica B* **180-181** 926-928
[23] Andersen K H, Stirling W G, Scherm R, Stunault A, Fak B, Godfrin H and Dianoux A J 1992 *Physica B* **180-181** 851-853
[24] Lauter H-J, Godfrin H, Frank V L P and Leiderer P 1992 *Phys. Rev. Lett.* **68** 2484
[25] Lauter H J, Godfrin H, Frank V L P and Schildberg H P 1990 *Physica B* **165-166** 597-598
[26] Hernandez E S and Calbi M M 2000 *J. Low Temp. Phys.* **120** 1